

## SYNTHESIS OF MAGNETIC NANOPARTICLES OF $\text{TiO}_2\text{-NiFe}_2\text{O}_4$ : CHARACTERIZATION AND PHOTOCATALYTIC ACTIVITY ON DEGRADATION OF RHODAMINE B

Rahmayeni\*, Syukri Arief, Yeni Stiadi, Rianda Rizal, and Zulhadjri

Department of Chemistry, Faculty of Mathematics and Natural Sciences,  
University of Andalas, Kampus Limau Manis, Padang 25163, West Sumatera-Indonesia

Received June 25, 2012; Accepted October 29, 2012

### ABSTRACT

Magnetic nanoparticles of  $\text{TiO}_2\text{-}(x)\text{NiFe}_2\text{O}_4$  with  $x = 0.01, 0.1, \text{ and } 0.3$  have been synthesized by mixture of titanium isopropoxide (TIP) and nitric metal as precursors. The particles were characterized by XRD, SEM-EDX, and VSM. XRD pattern show the peaks at  $2\theta = 25.3^\circ, 38.4^\circ$  and  $47.9^\circ$  which are referred as anatase phase of  $\text{TiO}_2$ . Meanwhile  $\text{NiFe}_2\text{O}_4$  phase was observed clearly for  $x = 0.3$ . The present of  $\text{NiFe}_2\text{O}_4$  can prevent the transformation of  $\text{TiO}_2$  from anatase to rutile when the calcination temperature increased. Microstructure analyses by SEM show the homogeneous form and size of particles. The magnetic properties analysis by VSM indicates that  $\text{TiO}_2\text{-NiFe}_2\text{O}_4$  is paramagnetic behavior.  $\text{TiO}_2$  doped  $\text{NiFe}_2\text{O}_4$  has higher photocatalytic activity than  $\text{TiO}_2$  synthesized for degradation of Rhodamine B in aqueous solution under solar light irradiation.

**Keywords:**  $\text{TiO}_2\text{-NiFe}_2\text{O}_4$ ; magnetic properties; photocatalytic activity; Rhodamine B

### ABSTRAK

Nanopartikel magnetik  $\text{TiO}_2\text{-}(x)\text{NiFe}_2\text{O}_4$  dengan  $x = 0,01, 0,1, \text{ dan } 0,3$  telah disintesis dengan menggunakan campuran titanium isopropoksida (TIP) dan logam nitrat sebagai prekursor. Partikel dikarakterisasi dengan menggunakan XRD, SEM-EDX, dan VSM. Pola XRD memperlihatkan puncak-puncak pada  $2\theta = 25,3^\circ, 38,4^\circ, \text{ dan } 47,9^\circ$  yang merupakan puncak dari  $\text{TiO}_2$  dalam fasa anatase. Sementara fasa  $\text{NiFe}_2\text{O}_4$  teramati dengan jelas untuk  $x = 0,3$ . Adanya  $\text{NiFe}_2\text{O}_4$  dapat menahan perubahan  $\text{TiO}_2$  dari anatase ke rutil ketika temperatur kalsinasi dinaikkan. Analisis mikrostruktur dengan SEM memperlihatkan bentuk dan ukuran partikel yang homogen. Analisis sifat magnetik dengan VSM memperlihatkan bahwa  $\text{TiO}_2\text{-NiFe}_2\text{O}_4$  bersifat paramagnetik.  $\text{TiO}_2$  yang didoping dengan  $\text{NiFe}_2\text{O}_4$  mempunyai sifat aktivitas fotokatalitik yang lebih tinggi dibanding dengan  $\text{TiO}_2$  yang disintesis terhadap degradasi senyawa Rhodamin B dalam larutan berair di bawah radiasi sinar matahari.

**Kata Kunci:**  $\text{TiO}_2\text{-NiFe}_2\text{O}_4$ ; sifat magnetik; aktivitas fotokatalitik; Rhodamin B

### INTRODUCTION

Metal oxide semiconductor photocatalysts, mainly  $\text{TiO}_2$  have generated high interest of chemists due to their potential in degradation of organic and inorganic pollutant in air or water [1]. There are several reasons using of  $\text{TiO}_2$  as photocatalyst such as: high activity, chemical stability, non toxic, low in cost, commercial availability, non corrosive, etc [2-3]. Usually,  $\text{TiO}_2$  is used as thin film coated on the surface of fiber glass, steel plate, plastic and so on, in order to be recovered easily, however its photoactivity is highly decreased since the effective surface area of photocatalysts is decreased considerably. In the water and waste water treatment,  $\text{TiO}_2$  has high specific surface area and good dispersion when it is used as powder or slurry but difficult in recycling for the next usage [1,4].

Recently, the demand of visible-light activated photo catalytic system increases rapidly; eventhough, the efficiency and availability of photocatalysts which can be activated by solar irradiation and indoor lighting is limited [2]. The majorities of current photocatalyst system use pure  $\text{TiO}_2$  with a metastable anatase crystal structure or  $\text{TiO}_2$ -modified.  $\text{TiO}_2$  is active only under ultraviolet light ( $\lambda < 400 \text{ nm}$ ) since its wide band gap of 3.2 eV (for the crystalline anatase phase).  $\text{TiO}_2$  utilizes less than 5% of solar spectrum and virtually none of light commonly used for indoor illumination [2,4-5].

The attempts toward extending the photoresponse of  $\text{TiO}_2$  to visible wavelengths are increasing exponentially every year. The most successful methods used to the development of modified  $\text{TiO}_2$  for visible light photocatalysts are implantation methods using Cr or V ions [6], deposit Ag

\* Corresponding author. Tel/Fax : +62-751-791410  
Email address : rahmayenni83@yahoo.com

on  $\text{TiO}_2$  [7],  $\text{TiO}_2$  doped Ag [8], doping nonmetals (N and P) [9], doping metal oxide such as  $\text{Fe}_2\text{O}_3$  [10-11], and various synthesis techniques.

The magnetic  $M\text{Fe}_2\text{O}_4$  nanoparticles ( $M$  = transition metals) such as  $\text{ZnFe}_2\text{O}_4$  with narrow band gap (1.9 eV) can be used to increase the photocatalytic effect of  $\text{TiO}_2$  in visible light [12].  $\text{TiO}_2$  doped by  $\text{ZnFe}_2\text{O}_4$  in certain ratio reduce the band gap and increase the photocatalytic activity in visible light. It is interesting to synthesize another doping as  $\text{TiO}_2$ - $M\text{Fe}_2\text{O}_4$  and observe their effect on photocatalytic activity [2,4]. For this purpose, we have reported the synthesis  $M\text{Fe}_2\text{O}_4$  and  $\text{TiO}_2$  doped by  $\text{CoFe}_2\text{O}_4$  and determined their photocatalytic activities toward degradation of organic compounds [13-14].

In this paper we report the preparation of magnetic nanoparticles photocatalysts  $\text{TiO}_2$ - $\text{NiFe}_2\text{O}_4$  that response to visible and solar light irradiation. These materials have magnetic behavior. Photocatalytic activity was determined by Rhodamine B degradation in aqueous solution under solar light irradiation.

## EXPERIMENTAL SECTION

### Materials

The materials used in this research were titanium isopropoxide (TIP) 97% (Sigma-Aldrich),  $\text{Ni}(\text{NO}_3)_2 \cdot 6\text{H}_2\text{O}$  (Merck),  $\text{Fe}(\text{NO}_3)_3 \cdot 9\text{H}_2\text{O}$  98% (Merck), ethanol p.a, 1-propanol p.a, isopropanol p.a (Merck), aquadest, ammonia, citric acid, and Rhodamine B.

### Instrumentation

The instruments used were X-ray diffraction (XRD Philips PW 1710), scanning electron microscopy (SEM JEOL JSM-6360LA), energy dispersive X-ray (EDX), vibrating sample magnetometer (VSM OXFORD 1.2H), and UV-Vis spectrophotometer.

### Procedure

#### Preparation of magnetic $\text{TiO}_2$ - $\text{NiFe}_2\text{O}_4$ nanoparticles

The magnetic  $\text{TiO}_2$ - $(x)\text{NiFe}_2\text{O}_4$  nanoparticles with  $x$  (mole fraction) values at 0.01, 0.1, and 0.3 were prepared using titanium isopropoxide (TIP) and nitric metal as precursors. Both of  $\text{Fe}(\text{NO}_3)_3 \cdot 9\text{H}_2\text{O}$  and  $\text{Ni}(\text{NO}_3)_2 \cdot 6\text{H}_2\text{O}$  was diluted into three types of alcohol (ethanol, propanol, isopropanol) to obtain 0.05 M nitric metal solutions. The solutions were heated at 65 °C with constant stirring for 30 minutes. In order to increase the pH of the mixture to 6.5,  $\text{NH}_4\text{OH}$  in alcohol 2 M was added into the mixture and followed by 10 mL aquadest that was added drop-wise. Then, the mixture was stirred for 45 min. A solution of TIP and alcohol was mixed in

ratio 1 : 2 that was prepared separately was added drop wise to the mixture and stirring was continued for 90 min. The mixture was dried at 120 °C for 24 h. Finally, the samples were calcined at 450, 500, 550, and 600 °C for 3 h. The nanoparticles were characterized by X-ray diffraction (XRD Philips PW 1710), scanning electron microscopy (SEM JEOL JSM-6360LA), energy dispersive X-ray (EDX) and vibrating sample magnetometer (VSM OXFORD 1.2H).

#### Preparation of $\text{NiFe}_2\text{O}_4$ nanoparticles

For the purpose of comparison,  $\text{NiFe}_2\text{O}_4$  nanoparticles were prepared by sol gel process. Nitric salts of Fe and Ni were dissolved in ethanol to get the 1.0 M nitric metal solutions.  $\text{Fe}(\text{NO}_3)_3 \cdot 9\text{H}_2\text{O}$  and  $\text{Ni}(\text{NO}_3)_2 \cdot 6\text{H}_2\text{O}$  solution were mixed in 1 : 2 mole ratio for  $\text{Ni}^{2+} : \text{Fe}^{3+}$ . Citric acid was added slowly into the mixture until the mole ratio of  $M : \text{citric acid}$  is 1 : 1.5 ( $M$  = the mixture of  $\text{Fe}^{3+}$  and  $\text{Ni}^{2+}$ ). After that, the solution was heated to 70 °C for 1 h under vigorous stirring to allow evaporation to form a gel. Furthermore, the gel was dried at 120 °C for 24 h. Finally, the dry gel was calcined at 600 °C in a furnace for 2 h and cooled to room temperature. The obtained nanoparticles were characterized by XRD [13].

#### Photocatalytic activity of magnetic $\text{TiO}_2$ - $\text{NiFe}_2\text{O}_4$ nanoparticles

Photocatalytic activity of magnetic  $\text{TiO}_2$ - $(x)\text{NiFe}_2\text{O}_4$  nanoparticles with  $x = 0.01, 0.1, \text{ and } 0.3$  was determined by degradation Rhodamine B compound that exposed under solar light irradiation. Amount of Rhodamine B was dissolved in distilled water to get 5 ppm solution. Then, 0.02 g of  $\text{TiO}_2$ - $\text{NiFe}_2\text{O}_4$  nanoparticles was added to 20 mL of the solution and then the mixture was exposed under solar light irradiation for 1, 2, and 3 h. After that the mixture was separated by centrifuge and the absorbance of solution was measured by UV-vis spectrophotometer to obtain the degradation percentage of Rhodamine B.

## RESULT AND DISCUSSION

### SEM-EDX Observation

The microstructure of  $\text{TiO}_2$ - $(x)\text{NiFe}_2\text{O}_4$  were investigated by scanning electron microscopy (SEM) in order to observe the morphology of nanoparticles. Fig. 1 shows SEM images of  $\text{TiO}_2$ - $(x)\text{NiFe}_2\text{O}_4$  nanoparticles with  $x = 0.01$  that calcined at 500 °C using propanol as solvent. It can be seen that the particles uniform a small granules shape with a smooth surface in the size of range between 0.075 to 0.25  $\mu\text{m}$ . These shapes are very beneficial toward photocatalytic properties due to the smaller particle size giving a larger surface area of

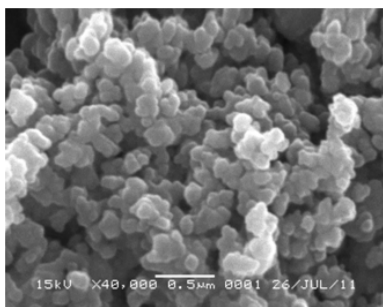


**Fig 1.** SEM image of  $\text{TiO}_2\text{-(x)NiFe}_2\text{O}_4$  with  $x = 0.01$  using propanol solvent and calcined at  $500\text{ }^\circ\text{C}$

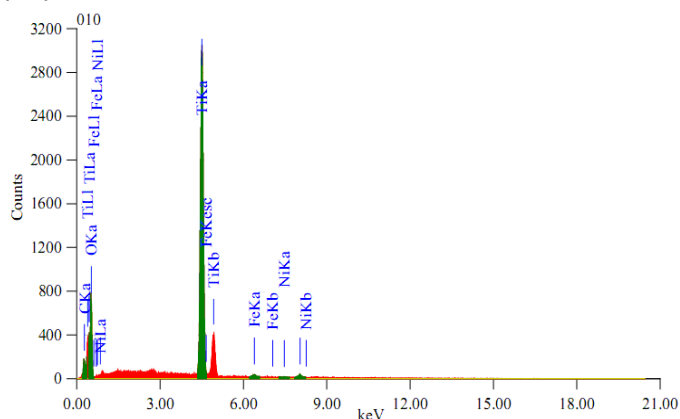


**Fig 3.** EDX analysis of  $\text{TiO}_2\text{-(x)NiFe}_2\text{O}_4$  nanoparticles for  $x = 0.01$  calcined at  $500\text{ }^\circ\text{C}$  with propanol as solvent

catalyst and corresponding to increase the photocatalytic activity of particles. The small white particle is also observed in the Fig. 1 which is predicted as  $\text{NiFe}_2\text{O}_4$  doped into  $\text{TiO}_2$ . In addition, there are also many pores observed in the image which could increase the catalytic activity.

Fig. 2 shows SEM images of  $\text{TiO}_2\text{-NiFe}_2\text{O}_4$  with  $x = 0.01$  and the calcination temperature of  $500\text{ }^\circ\text{C}$  with variation of solvent: (a) ethanol, (b) propanol, and (c) isopropanol. It can be seen that the surface of  $\text{TiO}_2\text{-NiFe}_2\text{O}_4$  using the propanol solvent is more homogeneous and regularity in particle size compared with the other particles prepared by ethanol and isopropanol solvents. The particle sizes of the propanol solvent product are also smaller compared with the others.

The composition of elements in  $\text{TiO}_2\text{-NiFe}_2\text{O}_4$  was analyzed by EDX and the results for  $x = 0.01$  with  $500\text{ }^\circ\text{C}$  of calcination temperature and propanol as solvent are shown in Fig. 3. There are three elements Ti, Ni, and Fe observed in the sample with composition percentage 24.25, 0.04 and 0.25%, respectively. These results are in agreement with the calculation of each element of Ti, Ni, and Fe in  $\text{TiO}_2\text{-NiFe}_2\text{O}_4$ .

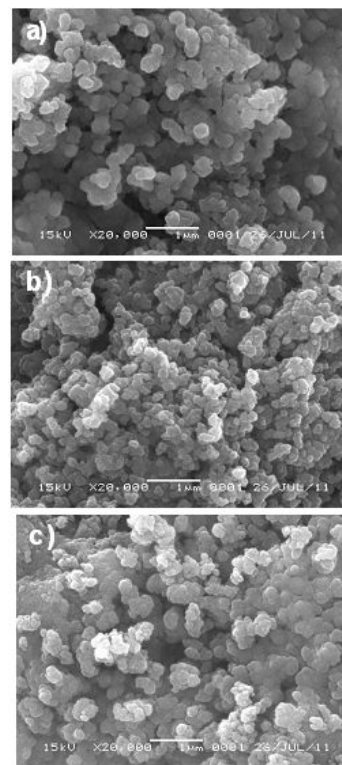


**Fig 2.** SEM image of  $\text{TiO}_2\text{-(x)NiFe}_2\text{O}_4$  with  $x = 0.01$ , calcined at  $500\text{ }^\circ\text{C}$  with different solvents a). Ethanol, b). Propanol, and c). Isopropanol

### X-ray Diffraction Analysis

Fig. 4 shows the XRD patterns of  $\text{TiO}_2\text{-(x)NiFe}_2\text{O}_4$  nanoparticles for  $x = 0.01$  with various calcination temperatures  $450, 500, 550,$  and  $600\text{ }^\circ\text{C}$ . All samples show the same pattern and considered as  $\text{TiO}_2$  anatase since the main peaks of  $2\theta = 25.3^\circ, 38.4^\circ$  and  $47.9^\circ$  corresponding to the JCPDS no. 21-1272. The peaks of  $\text{Ni}_2\text{Fe}_2\text{O}_4$  do not appear in these patterns. The increases of calcination temperature show the changes in the intensity of anatase  $\text{TiO}_2$ . The anatase intensity increases with increasing of temperature calcination from  $450$  to  $550\text{ }^\circ\text{C}$  and decrease at  $600\text{ }^\circ\text{C}$  by forming of rutile phase. In the inset a) can be seen that the highest intensity of anatase phase obtained at calcination temperature of  $550\text{ }^\circ\text{C}$ . Inset b) shows the phase transformation of  $\text{TiO}_2$  anatase to rutile which is observed at  $2\theta = 36 - 40^\circ$ . The rutile phase appears at temperature above  $550\text{ }^\circ\text{C}$  for  $\text{TiO}_2$  doped  $\text{NiFe}_2\text{O}_4$ . However, it is obtained at  $500\text{ }^\circ\text{C}$  for the  $\text{TiO}_2$  synthesized (prepared by sol gel process) without  $\text{NiFe}_2\text{O}_4$ . It can be concluded that the present of  $\text{NiFe}_2\text{O}_4$  can prevent the transformation of  $\text{TiO}_2$  from anatase to rutile phases as the calcination temperature increased.

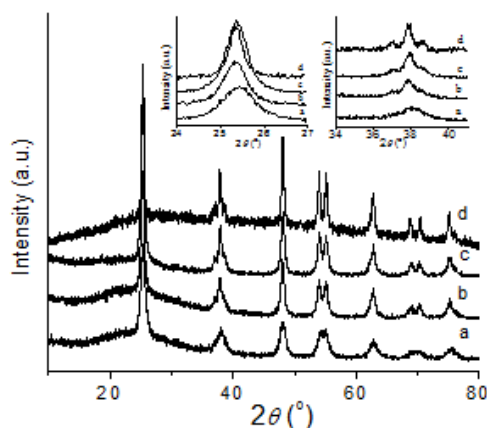


**Fig 4.** XRD patterns of  $\text{TiO}_2\text{-(x)NiFe}_2\text{O}_4$  nanoparticles for  $x = 0.01$  with various calcination temperatures a) 450, b) 500, c) 550, and d) 600 °C. The insets show the peaks around  $2\theta$  at a) 25° and b) 38°

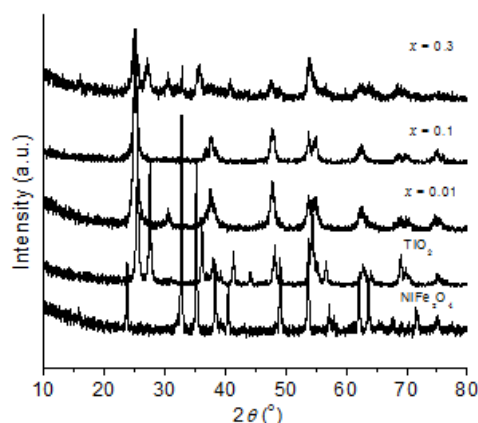


**Fig 5.** XRD patterns of  $\text{TiO}_2\text{-(x)NiFe}_2\text{O}_4$  calcined at 500 °C for  $x = 0.01, 0.1,$  and  $0.3$  including XRD patterns of  $\text{NiFe}_2\text{O}_4$  and  $\text{TiO}_2$  synthesized as references

The particle size of  $\text{TiO}_2\text{-NiFe}_2\text{O}_4$  was calculated by using Debye-Scherrer formula. The results are 8.07, 9.68, 13.98, and 21.47 nm for the calcination temperature at 450, 500, 550 and 600 °C, respectively. It means that the increasing of calcination temperature give increasing of particle size of the samples.

Fig. 5 shows the XRD patterns of  $\text{TiO}_2$  with variation of  $\text{NiFe}_2\text{O}_4$  concentration ( $x = 0.01, 0.1,$  and  $0.3$ ) calcined at 500 °C. For the samples with the  $x = 0.01$  and  $0.1$ , the patterns show only the anatase phase. There is no  $\text{NiFe}_2\text{O}_4$  observed due to its concentration is quite small. However, for  $x = 0.3$ , the patterns of XRD show both of anatase and rutile phase. Increasing of  $\text{NiFe}_2\text{O}_4$  concentration changed a part of the anatase phase to rutile. This pattern also shows the  $\text{NiFe}_2\text{O}_4$  phase indicated by the  $2\theta = 32.42^\circ$  and  $35.59^\circ$ . These results are in agreement with the XRD patterns of  $\text{NiFe}_2\text{O}_4$  and  $\text{TiO}_2$  synthesized.

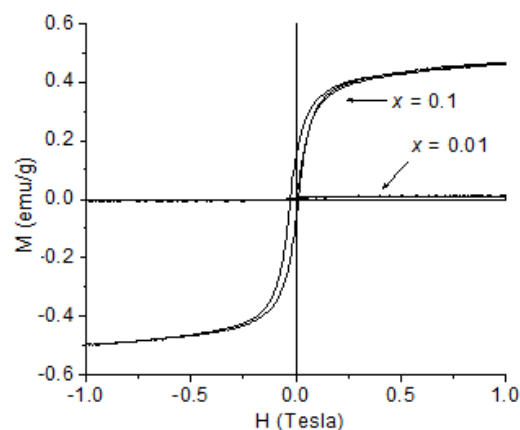


**Fig 6.** Magnetic properties of  $\text{TiO}_2\text{-(x)NiFe}_2\text{O}_4$  nanoparticles with  $x = 0.01$  and  $0.1$

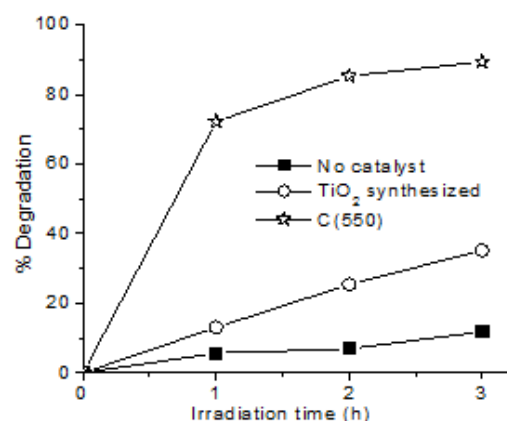


**Fig 7.** Photocatalytic activity of  $\text{TiO}_2\text{-(x)NiFe}_2\text{O}_4$  with  $x = 0.01$ ,  $\text{TiO}_2$  synthesized calcined at 500 °C, and absence catalysts on degradation of Rhodamine B under solar light irradiation

### Magnetic Characterization

The magnetic properties of  $\text{TiO}_2\text{-(x)NiFe}_2\text{O}_4$  nanoparticles for  $x = 0.01$  and  $0.1$  calcined at 500 °C were measured by VSM and the results are shown in Fig. 6. The magnetic properties of sample with  $x = 0.01$  shows a soft interaction to the magnetic field applied. These indicate a weak interaction of spin magnetic in the sample and referred to the diamagnetic properties. On the other hands, the sample with  $x = 0.1$  shows a stronger magnetic interaction indicated by the high of magnetization with the value 0.462 emu/g at 0.99 T magnetic field and the coercive and remanent value at  $-0.0061$  T and  $0.003$  emu/g, respectively. These results correspond to the paramagnetic properties. It can be concluded that magnetization value of  $\text{TiO}_2\text{-NiFe}_2\text{O}_4$  nanoparticles increases with increasing the concentration of  $\text{NiFe}_2\text{O}_4$  in  $\text{TiO}_2$ . The catalysts containing magnetic properties gain profit due to easier

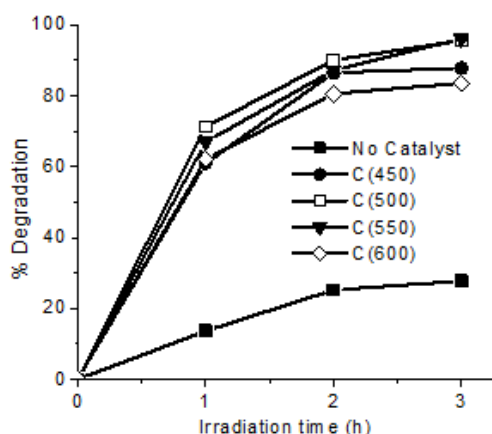


**Fig 8.** Photocatalytic activity of  $\text{TiO}_2\text{-NiFe}_2\text{O}_4$  nanoparticles with  $x = 0.01$  calcined at temperature 450, 500, 550, and 600 °C on degradation of Rhodamine B under solar light irradiation

in separating and can be reused for the several time.

#### Photocatalytic Activity of $\text{TiO}_2\text{-NiFe}_2\text{O}_4$ Nanoparticles

Fig. 7 shows the photocatalytic activity of  $\text{TiO}_2\text{-(x)NiFe}_2\text{O}_4$  nanoparticles in response to visible or solar light. They were carried out by degradation of Rhodamine B solution under solar light irradiation along 1, 2, and 3 h. These figure show only for the sample with  $x = 0.01$  calcined at 500 °C and compared with the  $\text{TiO}_2$  and absence of catalysts. The catalytic activities of the samples are around 90% for 3 h. These results are better than  $\text{TiO}_2$  synthesized and absence of catalysts with the percentage of degradation is around 30%, and 10% respectively with the same time. It can be concluded that the presence of  $\text{NiFe}_2\text{O}_4$  in  $\text{TiO}_2$  can enhance the photocatalytic activity with the result that it can adsorb effectively the visible and solar light. It is predicted that the presence of  $\text{NiFe}_2\text{O}_4$  can make a shorter of the band gap of  $\text{TiO}_2$  giving effect to the long life time of the electron in conduction band and prevent it to recombine into the electron hole fastly.

Fig. 8 shows the curve of photocatalytic activity of  $\text{TiO}_2\text{-(x)NiFe}_2\text{O}_4$  nanoparticles with  $x = 0.01$  calcined at 450, 500, 550, and 600 °C on degradation of Rhodamine B under solar light irradiation. The activities of catalysts increase with the increasing of the long time of light irradiation. The good activities are shown by catalysts calcined at 500 and 550 °C with percentage degradation 89.34% and 85.39% for 3 h, respectively. However the sample calcined at 600 °C show slightly decreasing of activities catalytic. This is in agreement with the transition of phase since the rutile phase initiated to form.

Influence the amount of metal oxide to the photocatalytic effect can be seen in Fig. 9. At  $x = 0.1$

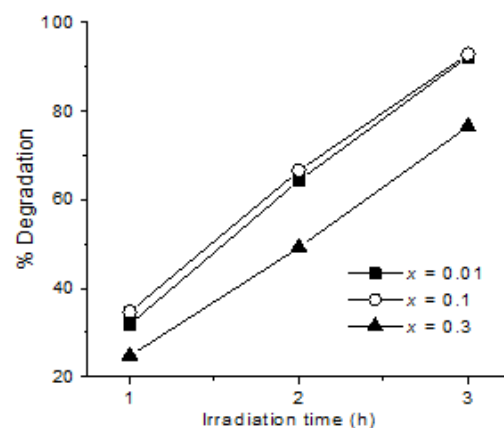


**Fig 9.** Photocatalytic activity of  $\text{TiO}_2\text{-(x)NiFe}_2\text{O}_4$  nanoparticles with  $x = 0.01$ , 0.1, and 0.3 on degradation of Rhodamine B under solar light irradiation

gives a better photocatalytic effect than the  $x = 0.01$  and  $x = 0.3$ . At concentrations higher metal oxides decreased percent degradation of Rhodamine B compound. This is due to the phase in  $\text{TiO}_2\text{-anatase}$  in  $\text{TiO}_2\text{-NiFe}_2\text{O}_4$  at higher concentrations of  $\text{NiFe}_2\text{O}_4$  begun to change into rutile.

The effect of  $\text{NiFe}_2\text{O}_4$  concentration ( $x = 0.01$ , 0.1, and 0.3) in catalyst  $\text{TiO}_2$  toward photocatalytic activities are shown in Fig. 9. From this figure, it can be seen that the sample with  $x = 0.1$  shows a better photocatalytic effect compared with the  $x = 0.01$  and 0.3, however the catalysts with  $x = 0.3$  shows lower activities compared with  $x = 0.01$ . Increasing  $\text{NiFe}_2\text{O}_4$  concentration can increase the catalytic activity until  $x = 0.1$ . On the other hand increasing more  $\text{NiFe}_2\text{O}_4$  concentration until  $x = 0.3$  reduce catalytic activity. It can be concluded that catalytic activity is given mainly by  $\text{TiO}_2$ . Introducing the high of  $\text{NiFe}_2\text{O}_4$  as magnetic properties material into  $\text{TiO}_2$  phase can decrease the catalytic activity of  $\text{TiO}_2$  and change the anatase to rutile phases. Rutile phase is not effective in responding to the visible and solar light.

Compared the percentage degradation of Rhodamine B in Fig. 7, 8, and 9, the percentage degradation in Fig. 9 is around 35% for 1 h and lower than the Fig. 7 and 8 both also in 1 h with the value around 75%. The different of these results can be predicted due to the intensity of solar light not equal in every day although treated on the same time.

#### CONCLUSION

In order to develop a photocatalyst that can work in the visible and solar light,  $\text{TiO}_2\text{-(x)NiFe}_2\text{O}_4$  nanoparticles with  $x = 0.01$ , 0.1, and 0.3 have been synthesized by using nitric metal and titanium

isopropoxide as precursors. The present of  $\text{NiFe}_2\text{O}_4$  can prevent the transformation of  $\text{TiO}_2$  from anatase to rutile phases as the calcination temperature increased. SEM photographs showed the homogeneous particle shape with a uniform size of sample. The photocatalytic activities of  $\text{TiO}_2\text{-NiFe}_2\text{O}_4$  toward degradation of Rhodamine B in aqueous solution under solar light irradiation are better than  $\text{TiO}_2$ -synthesized.  $\text{TiO}_2\text{-NiFe}_2\text{O}_4$  nanoparticles show magnetic behavior and allowing this material be recycled from the water for subsequent in use.

#### ACKNOWLEDGEMENT

The authors wish to thank the Directorate General of Higher Education, Ministry Education and Culture Republic of Indonesia for supporting this work by Fundamental research no. 169/SP2H/PL/DitLitabmas/IV/2011, BATAN for XRD, SEM, and VSM facilities.

#### REFERENCES

1. Shihong, X.U., Wenfeng, S., Jian, Y., Mingxia, C., and Jianwei, S., 2007, *Chin. J. Chem. Eng.*, 15, 2, 190–195.
2. Srinivasan, S.S., Wade, J., and Stefanakos, E.K., 2006, *J. Nanomater.*, 45712, 1–4.
3. Hirotaka, N., Koichi, K., and Masashi, T., 2009, *J. Oleo Sci.*, 58, 7, 389–394.
4. Zhang, B., Zhang, J., and Chen, F., 2008, *Res. Chem. Intermed.*, 34, 4, 375–380.
5. Jeong, E.D., Borse, P.H., Jang, J.S., Lee, J.S., Jung, O-K., Chang, H., Jin, J.S., Won, M.S., and Kim, H.G., 2008, *J. Ceram. Process. Res.*, 9, 3, 250–253.
6. Anpo, M., 2000, *Stud. Surf. Sci. Catal.*, 130 A, 157–166.
7. Tryba, B., Piszcz, M., and Morawski, A.W., 2010, *Open Mater. Sci. J.*, 4, 5–8.
8. Behpour, M., Ghoreishi, S.M., and Razavi, F.S., 2010, *Dig. J. Nanomater. Bios.*, 5, 2, 467–475.
9. Kometani, N., Fujita, A., and Yonezawa, Y., 2008, *J. Mater. Sci.*, 43, 2492–2498.
10. Rana, S., Srivastava, R.S., Soresson, M.M., and Misra, R.D.K., 2005, *Mater. Sci. Eng., B*, 119, 2, 144–151.
11. Beydoun, D., and Amal, R., 2002, *Mater. Sci. Eng., B*, 94, 1, 71–81.
12. Meng, W., Li, F., Evans, D.G., and Duan, X., *J. Porous Mater.*, 11, 2, 97–105.
13. Rahmayeni, Syukri, A., Yeni, S., and Herlin, O., 2010, *J. Chem. Res.*, 4, 1, 55–61.
14. Rahmayeni, Upita, S., Syukri, A., and Hayatul, H., 2011, *J. Chem. Res.*, 4, 2, 71–78.